Tech Science Press

Dual Branches of MHD Three-Dimensional Rotating Flow of Hybrid Nanofluid on Nonlinear Shrinking Sheet

Liaquat Ali Lund[1,2,*], Zurni Omar[1], Ilyas Khan[3] and El-Sayed M. Sherif[4,5]

[1]School of Quantitative Sciences, Universiti Utara Malaysia, Sintok, Kedah, 06010, Malaysia
[2]KCAET Khairpur Mir's, Sindh Agriculture University, Tandojam, Sindh, 70060, Pakistan
[3]Faculty of Mathematics and Statistics, Ton Duc Thang University, Ho Chi Minh City, Vietnam
[4]Center of Excellence for Research in Engineering Materials, King Saud University, Al-Riyadh, 11421, Saudi Arabia
[5]Electrochemistry and Corrosion Laboratory, Department of Physical Chemistry, National Research Centre, Dokki, Cairo, 12622, Egypt
*Corresponding Author: Liaquat Ali Lund. Email: balochliaqatali@gmail.com

Abstract: In this study, magnetohydrodynamic (MHD) three-dimensional (3D) flow of alumina (Al_2O_3) and copper (Cu) nanoparticles of an electrically conducting incompressible fluid in a rotating frame has been investigated. The shrinking surface generates the flow that also has been examined. The single-phase (i.e., Tiwari and Das) model is implemented for the hybrid nanofluid transport phenomena. Results for alumina and copper nanomaterials in the water base fluid are achieved. Boundary layer approximations are used to reduce governing partial differential (PDEs) system into the system of the ordinary differential equations (ODEs). The three-stage Lobatto IIIa method in *bvp4c* solver is applied for solutions of the governing model. Graphical results have been shown to examine how velocity and temperature fields are influenced by various applied parameters. It has been found that there are two branches for certain values of the suction/injection parameter b. The rise in copper volumetric concentration improved the velocity of hybrid nanofluid in the upper branch. The heat transfer rate improved for the case of hybrid nanofluid as compared to the viscous fluid and simple nanofluid.

Keywords: Nonlinear surface; viscous dissipation; MHD; Hybrid nanofluid; two branches

1 Introduction

A modern procreation liquid of strong thermal efficiency is useful in fulfilling industrial and technical needs. In the past, Choi et al. [1] developed nano-liquids and revealed that nanoparticles dispersion can improve the normal fluids' thermal conductivity. At present, dispersions of nanoparticles have been highly discussed topics for sophisticated heat engineering owing to their exceptional efficiency and sub-phenomenon of this kind of employed liquid. Graphene is among nanomaterials that have gained more consideration owing to its high heat capacity and strong stability when distributed in traditional fluids

(ethylene glycol or water) with low thermal efficiency. Sheikholeslami et al. [2] numerically examined the 3D flow of nanofluid with the magnetic effect. Hayat et al. [3] analytically studied the radiative MHD flow of viscoelastic nanofluid and found that radiation helps to improve the thermal conductivity and temperature of the fluid. Articles of the implementations, formulation, and thermomechanical characteristics of hybrid nanofluids were already undertaken by the following researchers: Subhani et al. [4], Qi et al. [5] and Islam et al. [6].

Due to the importance and demand of the heat transfer rate, researchers have introduced a hybrid nanofluid. Hybrid nanofluid appears to be a mixture of the regular fluid, which are gas, ethylene glycol, water, a blend of water and ethylene glycol, and two distinct classes of nanomaterials, which are carbon materials, metals, and metal oxides. A model for analyzing the heat capacity of hybrid nanofluids specifically in carbon nanotubes has been established by Esfe et al. [7]. Carbon nanotubes were chosen for the processing of hybrid nanofluid because of their high effect on thermal performance. Copper and aluminum pairs are both commonly utilized in experimental and theoretical research of synthetic nanofluids. Al_2O_3 provides poor thermal conductivity; nonetheless, strong chemical action in alumina may preserve the durability of the hybrid nanofluid [8]. In addition, the computational analyses of hybrid nanofluid have been applied to the problem of boundary layer movement. Initially, the fluid flow on a stretching sheet with alumina-copper/water hybrid nanofluid has been considered in this paper [9]. They noticed that rise in heat transfer occurred at higher rates of nanomaterials volume fraction. Also, in a series of publications, Lund et al. [10–13] extended the problems of hybrid nanofluid flow to multiple physical effects, considering the multiple solutions. In addition, some scholars have also addressed the flow of hybrid nanofluid's problem along with specific physical conditions [14–17]. Besides, the usage of hybrid nanofluid will expand the heat rate attributed to the harmonious impacts mentioned by Sarkar et al. [18]. Owing to its potential to increase heat transfer rate, most utilizations involving heat transfer, like coolant in electronic and machining and transmitter conserving, regard hybrid nanofluid as heat transfer fluid.

The rotational 3D flow on the shrinking sheet coupled with the heat transfer rate has a huge application in biomedical, chemical, and manufacturing processes. Various uses of hybrid nanofluid are not possible without consideration of the effect of MHD. Recently, encouraging finding is the usage of MHD in cancer care drug targeting [19]. Hayat et al. [20] considered the 3D flow with the effect of MHD in rotational fluid flow on the stretching surface. They found that temperature reduced when Pr increased. Shah et al. [21] used the two-phase model of the nanofluid with the effect of Brownian motion in the rotating system. Hayat et al. [22] examined the nanofluid by using of the single-phase model with consideration of Darcy-Forchheimer porous medium effect.

The goal of this research is therefore to investigate the rotating angular effects of the hybrid nanofluid 3D flow across the magnetic field with viscous dissipation using the Tiwari et al. [23] models. To the best of the authors' knowledge, no such study has yet been considered. It can be said that this work is the extension of the work of Hayat et al. [20] and Hayat et al. [22] for the hybrid nanofluid on the nonlinear shrinking sheet where water is used as the base fluid, and alumina (first nanoparticles) and copper (second nanoparticles) are taken into account for hybrid nanomaterials. The findings are gotten for many applied parameters and described graphically. In addition, this whole theoretical framework would help several other engineers and scholars to explore the challenge facing the modern industry in terms of the rate of heat transfer and the need for coolant.

2 Mathematical Formulation

We have considered the steady, MHD, three-dimensional flow of hybrid nanofluid along with heat transfer past a flat plate. The sheet at $z = 0$ is shrinking nonlinearly in x-axis direction i.e., $u_w(x) = -cx^n$.

Mass flux of velocity is $v_w(x) = -b\sqrt{c\vartheta_f}x^{(n-1)/2}$, temperature within boundary layer is $T_w = T_\infty + T_0x^{2n}$ and outside the boundary layer is T_∞. Water and sheet both are rotating having angular velocity $\tilde{\Omega} = \Omega_0 x^{(1-n)}$ about the z-axis taken normal to the sheet. In z-direction, a uniform field of magnetic is placed, i.e., $B = B_0 x^{(1-n)/2}$. It results in magnetic effects in the x-axis and z-axis directions. The magnetic Reynolds number has been supposed very low and the field of induced magnetic has been ignored. Considering the momentum along with temperature boundary layers equations of hybrid nanofluid flow are described as

$$\frac{\partial u}{\partial x} + \frac{\partial v}{\partial y} + \frac{\partial w}{\partial z} = 0 \tag{1}$$

$$\left[u\frac{\partial}{\partial x} + v\frac{\partial}{\partial y} + w\frac{\partial}{\partial z}\right]u - 2\tilde{\Omega}v = -\frac{1}{\rho_{hnf}}\frac{\partial P}{\partial x} + \frac{\mu_{hnf}}{\rho_{hnf}}\left[\frac{\partial^2}{\partial x^2} + \frac{\partial^2}{\partial y^2} + \frac{\partial^2}{\partial z^2}\right]u - \frac{\sigma_{hnf}}{\rho_{hnf}}B^2u \tag{2}$$

$$\left[u\frac{\partial}{\partial x} + v\frac{\partial}{\partial y} + w\frac{\partial}{\partial z}\right]v - 2\tilde{\Omega}u = -\frac{1}{\rho_{hnf}}\frac{\partial P}{\partial y} + \frac{\mu_{hnf}}{\rho_{hnf}}\left[\frac{\partial^2}{\partial x^2} + \frac{\partial^2}{\partial y^2} + \frac{\partial^2}{\partial z^2}\right]v - \frac{\sigma_{hnf}}{\rho_{hnf}}B^2v \tag{3}$$

$$\left[u\frac{\partial}{\partial x} + v\frac{\partial}{\partial y} + w\frac{\partial}{\partial z}\right]w = -\frac{1}{\rho_{hnf}}\frac{\partial P}{\partial z} + \frac{\mu_{hnf}}{\rho_{hnf}}\left[\frac{\partial^2}{\partial x^2} + \frac{\partial^2}{\partial y^2} + \frac{\partial^2}{\partial z^2}\right]w \tag{4}$$

$$\left(\rho c_p\right)_{hnf}\left[u\frac{\partial}{\partial x} + v\frac{\partial}{\partial y} + w\frac{\partial}{\partial z}\right]T = k_{hnf}\left[\frac{\partial^2}{\partial x^2} + \frac{\partial^2}{\partial y^2} + \frac{\partial^2}{\partial z^2}\right]T + \Phi \tag{5}$$

The related boundary conditions (BCs) of Eqs. (1)–(5) are

$$\begin{cases} v = v_w(x), u = u_w(x), w = 0, T = T_w \quad at\, z = 0 \\ \quad u \to 0, v \to 0, T \to T_\infty, \quad as\, z \to \infty \end{cases} \tag{6}$$

where u, v, and w are the respective components of velocity in x, y and z-axes directions, σ_{hnf} is the electrical conductivity of the hybrid nanofluid, and P is the modified pressure including the centrifugal force term. Further, $\left(\rho c_p\right)_{hnf}$, μ_{hnf}, k_{hnf} and, ρ_{hnf} are the corresponding heat capacity, dynamic viscosity, thermal conductivity, and density of hybrid nanofluid. Moreover, subscript hnf shows the thermophilic properties of hybrid nanofluid. Further, the viscous dissipation function can be expressed as Φ.

$$\Phi = 2\mu_{hnf}\left[\left(\frac{\partial u}{\partial x}\right)^2 + \left(\frac{\partial v}{\partial y}\right)^2 + \left(\frac{\partial w}{\partial z}\right)^2 + \frac{1}{2}\left(\frac{\partial v}{\partial x} + \frac{\partial u}{\partial y}\right)^2 + \frac{1}{2}\left(\frac{\partial w}{\partial y} + \frac{\partial v}{\partial z}\right)^2 + \frac{1}{2}\left(\frac{\partial u}{\partial z} + \frac{\partial w}{\partial x}\right)^2\right]$$

The thermophysical properties are given in Tabs. 1–2.

We will employ similarity variables (7) in Eqs. (1)–(5) in order to obtain similarity solutions.

$$\begin{cases} u = cx^n f'(\eta), v = cx^n g(\eta), \eta = z\sqrt{\frac{c(n+1)}{2\vartheta_f}}x^{(n-1)/2} \\ w = -\sqrt{\frac{c\vartheta_f(n+1)}{2}}x^{(n-1)/2}\left[f(\eta) + \frac{n-1}{n+1}\eta f'(\eta)\right] \\ \quad\quad \theta(\eta) = \frac{(T - T_\infty)}{(T_w - T_\infty)} \end{cases} \tag{7}$$

substitute Eq. (7) in (2)–(6), it is obtained

$$f''' + \xi_1\xi_2\left[ff'' - \frac{2n}{(n+1)}f'^2 + \frac{4\Omega}{(n+1)}g\right] - \frac{\sigma_{hnf}}{\sigma_f}\xi_2 Mf' = 0 \tag{8}$$

Table 1: Thermophysical features of hybrid nanofluid

Properties	Hybrid Nanofluid
Dynamic viscosity	$\mu_{hnf} = \dfrac{\mu_f}{\left(1 - \phi_{Al_2O_3}\right)^{2.5}\left(1 - \phi_{Cu}\right)^{2.5}}$
Density	$\rho_{hnf} = (1 - \phi_{Cu})\left[\left(1 - \phi_{Al_2O_3}\right)\rho_f + \phi_{Al_2O_3}\rho_{Al_2O_3}\right] + \phi_{Cu}\rho_{Cu}$
Thermal conductivity	$k_{hnf} = \dfrac{k_{Cu} + 2k_{nf} - 2\phi_{Cu}\left(k_{nf} - k_{Cu}\right)}{k_{Cu} + 2k_{nf} + \phi_{Cu}\left(k_{nf} - k_{Cu}\right)} \times \left(k_{nf}\right)$
	where $k_{nf} = \dfrac{k_{Al_2O_3} + 2k_f - 2\phi_{Al_2O_3}\left(k_f - k_{Al_2O_3}\right)}{k_{Al_2O_3} + 2k_f + \phi_{Al_2O_3}\left(k_f - k_{Al_2O_3}\right)} \times \left(k_f\right)$
Heat capacity	$\left(\rho c_p\right)_{hnf} = (1 - \phi_{Cu})\left[\left(1 - \phi_{Al_2O_3}\right)\left(\rho c_p\right)_f + \phi_{Al_2O_3}\left(\rho c_p\right)_{Al_2O_3}\right] + \phi_{Cu}\left(\rho c_p\right)_{Cu}$
Electrical conductivity	$\sigma_{hnf} = \dfrac{\sigma_{Cu} + 2\sigma_{nf} - 2\phi_{Cu}\left(\sigma_{nf} - \sigma_{Cu}\right)}{\sigma_{Cu} + 2\sigma_{nf} + \phi_{Cu}\left(\sigma_{nf} - \sigma_{Cu}\right)} \times \left(\sigma_{nf}\right)$
	where $\sigma_{nf} = \dfrac{\sigma_{Al_2O_3} + 2\sigma_f - 2\phi_{Al_2O_3}\left(\sigma_f - \sigma_{Al_2O_3}\right)}{\sigma_{Al_2O_3} + 2\sigma_f + \phi_{Al_2O_3}\left(\sigma_f - \sigma_{Al_2O_3}\right)} \times \left(\sigma_f\right)$

Table 2: The properties of thermo physical

Properties	Water (H_2O)	Copper (Cu)	Alumina (Al_2O_3)
$\rho\ (kg/m3)$	997.1	8933	3970
$c_p (J/kg\ K)$	4179	385	765
$k\ (W/m\ K)$	0.613	400	40
$\sigma(S/m)$	0.05	5.96×10^7	3.69×10^7
Pr	6.2		

$$g'' + \xi_1\xi_2\left[fg' - \frac{2n}{(n+1)}f'g - \frac{4\Omega}{(n+1)}f'\right] - \frac{\sigma_{hnf}}{\sigma_f}\xi_2 Mg = 0 \tag{9}$$

$$\frac{\left(k_{hnf}/k_f\right)\xi_3}{Pr}\theta'' + \theta'f - \frac{4n}{(n+1)}\theta f' + \frac{\xi_3}{\xi_2}Ec_1(f'')^2 + \frac{\xi_3}{\xi_2}Ec_2(g')^2 = 0 \tag{10}$$

Along with BCs

$$\begin{cases} f(0) = -b\sqrt{\frac{2}{n+1}}, f'(0) = -1, g(0) = 0, \theta(0) = 1 \\ f'(\eta) \to 0, g(\eta) \to 0 \ \ \theta(\eta) \to 0, \quad as\,\eta \to \infty \end{cases} \tag{11}$$

$$\begin{cases} \xi_1 = \left\{ (1 - \phi_{Cu}) \left[1 - \phi_{Al_2O_3} + \phi_{Al_2O_3} \left(\frac{\rho_{Al_2O_3}}{\rho_f} \right) \right] + \phi_{Cu} \left(\frac{\rho_{Cu}}{\rho_f} \right) \right\} \\ \xi_2 = (1 - \phi_{Cu})^{2.5} \left(1 - \phi_{Al_2O_3} \right)^{2.5} \\ \xi_3 = \dfrac{1}{\left\{ (1 - \phi_{Cu}) \left[1 - \phi_{Al_2O_3} + \phi_{Al_2O_3} \frac{(\rho c_p)_{Al_2O_3}}{(\rho c_p)_f} \right] + \phi_{Cu} \frac{(\rho c_p)_{Cu}}{(\rho c_p)_f} \right\}} \end{cases} \tag{12}$$

Here prime represents the differentiation of η, $M = \frac{\sigma_f B_0^2}{c \rho_f (n+1)}$ is the magnetic number, $Pr = \frac{\vartheta_f}{\alpha_f}$ is Prandtl, $\Omega = \frac{\Omega_0}{c}$ is constant dimensionless rotation parameter, $Ec_1 = Ec_2 = \frac{c^2 \rho_f}{T_0 (\rho c_p)_f}$ are the Eckert numbers, and b is the suction parameter ($b < 0$) and injection parameter ($b > 0$).

Coefficient of skin friction and local numbers of Nusselt are physical quantities of interest and described as follows.

$$C_{fx} = \frac{\mu_{hnf}}{\rho_f c^2} \left(\frac{\partial u}{\partial z} \right) |z = 0,$$

$$C_{fy} = \frac{\mu_{hnf}}{\rho_f} \left(\frac{\partial v}{\partial z} \right) |z = 0, Nu_x = -\frac{k_{hnf}}{k_f (T_w - T_\infty)} \left(\frac{\partial T}{\partial z} \right) |z = 0 \tag{13}$$

By substituting Eq. (7) in Eq. (14), it is obtained

$$2\sqrt{Re} C_{fx} = \frac{1}{\left(1 - \phi_{Al_2O_3} \right)^{2.5} (1 - \phi_{Cu})^{2.5}} f''(0); 2\sqrt{Re} C_{fy}$$

$$= \frac{1}{\left(1 - \phi_{Al_2O_3} \right)^{2.5} (1 - \phi_{Cu})^{2.5}} g'(0) \sqrt{\frac{Re}{2}} Nu_x \tag{14}$$

$$= -\frac{k_{hnf}}{k_f} \theta'(0)$$

where Re_x is the local Reynold number.

3 Results and Discussion

By using MATLAB program with its outstanding *bvp4c* function, similarity multiple branches have been gotten by solving Eqs. (8)–(10) along with BCs Eq. (11). This solver is made with help of a collocation technique that contains 4th order accuracy. The *bvp4c* solver will function reliably to forecast branches by employing the pair of random initial assumptions, yet, average processor time for computing results can vary based on the use of the original assumptions. The thickness of boundary layer $\eta_\infty = 8$, $Pr = 6.2$ (for water water at room temperature 25°C), the solid volume fraction of alumina $\phi_{Al_2O_3} = 0.1$ have been kept in the whole study, whereas appropriate initial assumptions for code of *bvp4c* and values of other physical quantities have been selected till the velocity and temperature profiles meet the BCs Eq. (11) asymptotically at $\eta \to \infty$. We have set the error of the relative tolerance 10^{-10} which is acceptable scientifically for the excellent accuracy. The system of governing Eqs. (8)–(10) are reduced as follows:

$$f = y(1); f' = y(2); f'' = y(3); g = y(4); g' = y(5); \theta = y(6); \theta' = y(7)$$

$$f''' = -\xi_1 \xi_2 \left[f f'' - \frac{2n}{(n+1)} f^{2'} + \frac{4\Omega}{(n+1)} g \right] - \frac{\sigma_{hnf}}{\sigma_f} \xi_2 M f'$$

$$= -\xi_1 \xi_2 \left[y(1) * y(3) - \frac{2 * n}{(n+1)} * y(1) * y(1) + \frac{4 * \Omega}{(n+1)} * y(4) \right] - \frac{\sigma_{hnf}}{\sigma_f} * \xi_2 * M * y(2) \tag{15}$$

$$g'' = -\xi_1\xi_2\left[fg' - \frac{2n}{(n+1)}f'g - \frac{4\Omega}{(n+1)}f'\right] - \frac{\sigma_{hnf}}{\sigma_f}\xi_2 Mg$$

$$= -\xi_1\xi_2\left[y(1)*y(5) - \frac{2*n}{(n+1)}*y(2)*y(4) - \frac{4*\Omega}{(n+1)}*y(2)\right] - \frac{\sigma_{hnf}}{\sigma_f}*\xi_2*M*y(4) \qquad (16)$$

$$\theta'' = \frac{-Pr}{(k_{hnf}/k_f)\xi_3}\left[\theta'f - \frac{4n}{(n+1)}\theta f' + \frac{\xi_3}{\xi_2}Ec_1(f'')^2 + \frac{\xi_3}{\xi_2}Ec_2(g')^2\right]$$

$$= \frac{-Pr}{(k_{hnf}/k_f)*\xi_3}\left[y(7)*y(1) - \frac{4*n}{(n+1)}*y(6)*y(2) + \frac{\xi_3}{\xi_2}*Ec_1*y(3)*y(3) + \frac{\xi_3}{\xi_2}*Ec_2*y(5)*y(5)\right] \qquad (17)$$

and BCs

$$ya(1) + b*\left(\frac{2}{n+1}\right)^{0.5}, \; ya(2) + 1, \; yb(2), \; ya(4), \; yb(4), \; ya(6) - 1, \; yb(6) \qquad (18)$$

where ya shows the initial condition and yb shows the far-field condition. The full description of the *bvp4c* solver can be read in Lund et al. [24,25].

Two branches of Eqs. (8)–(10) are noticed when $b \le b_c$ and no similarity branch could be found for $b > b_c$, as revealed in Figs. 1–7. Figs. 1–3 show the effect of ϕ_{Cu} on skin friction coefficient ($f''(0)$, $g'(0)$) and heat transfer rate ($-\theta'(0)$) against the various values of b. Two branches occur for the suction/injection parameter $b \le b_c$ where $b_{c1} = -2.4067$, $b_{c2} = -2.3004$ and $b_{c3} = -2.2272$ are the corresponding critical values of $\phi_{Cu} = 0.01$, 0.05 and 0.1. It should be noted that both branches exist at the point b_c. The first branch, magnitudes of $f''(0)$ and $g'(0)$ increase when ϕ_{Cu} is increased but reduce as the effect of suction goes toward to injection effect. On another side, the contrary pattern of $f''(0)$ and $g'(0)$ has been found in the lower branch. In Fig. 3, the magnitude of $-\theta'(0)$ is high when the volume fraction of the copper nanoparticles is 1% as compared to 5% and 10% in the upper branch. While the heat transfer rate increases when b enhances in the lower branch.
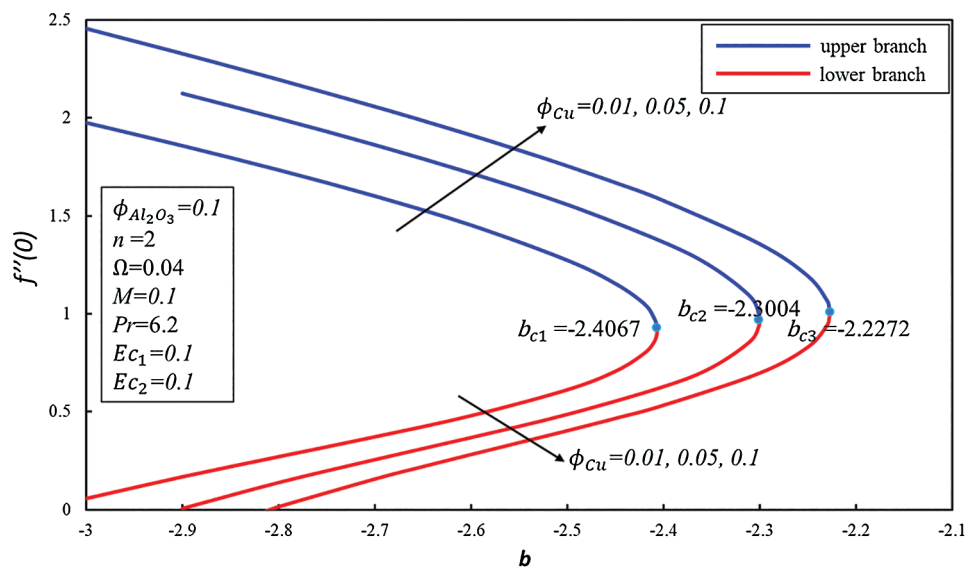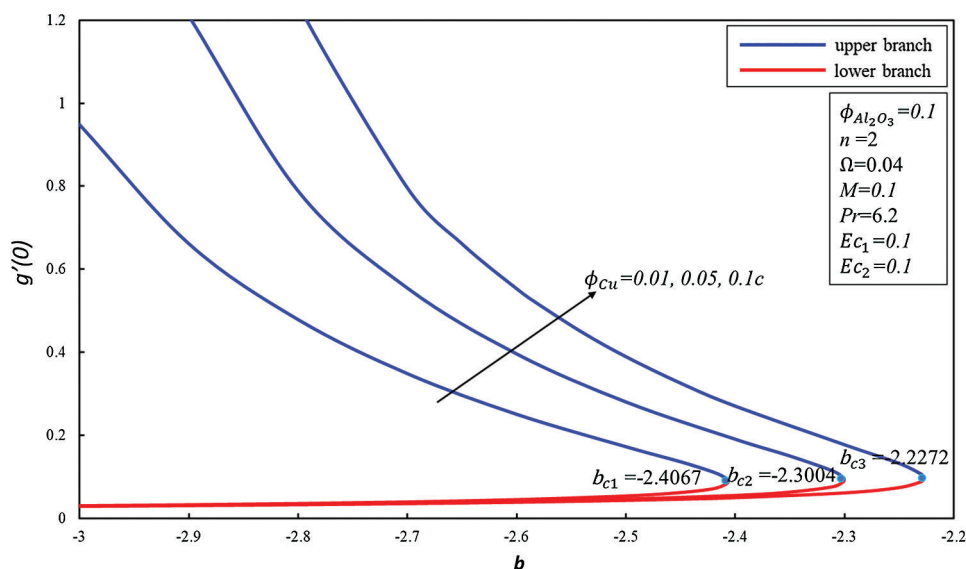

Figure 1: Effect of ϕ_{Cu} on $f''(0)$

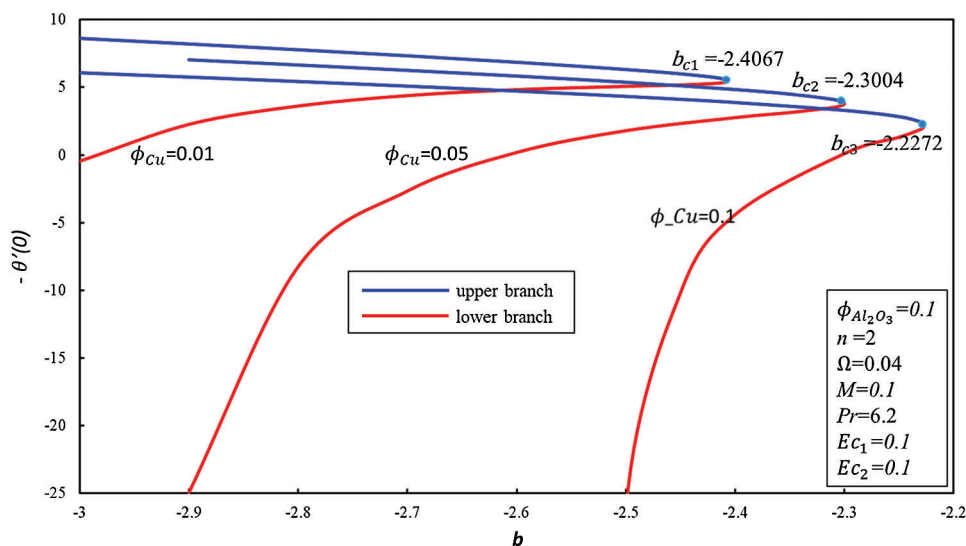**Figure 2:** Effect of ϕ_{Cu} on $g'(0)$

Figure 3: Effect of ϕ_{Cu} on $-\theta'(0)$

Fig. 4 shows the effect of M on profiles of velocity ($f'(\eta)$, $g(\eta)$) and temperature ($\theta(\eta)$). It is noticed that $f'(\eta)$, $g(\eta)$, and $\theta(\eta)$ decrease for the upper branch with the rise of M. The result is, however, inverted in the lower branch. It should be noted that singularity exists for in the lower branch of the temperature profile when $0.1 \leq M \leq 0.2$. Singularity indicates that the lower branch is unstable, therefore no need to perform the stability analysis in order to indicate the unstable branch. Logically, a magnetic field causes a Lorentz or drag force that involves reducing the movement of hybrid nanofluid.

Fig. 5 exemplifies that how the rotation parameter Ω affects the profiles of velocity ($f'(\eta)$, $g(\eta)$) and temperature ($\theta(\eta)$). In the upper branch, no change is noticed in $f'(\eta)$ and $\theta(\eta)$ profiles when Ω is enhanced. When growing the rotation parameter values Ω generates higher angular velocity $g(\eta)$ and higher momentum layer thickness in both branches. It should be noted that when $\Omega = 0.1$, we have

obtained a single branch only. For the lower branch of $\theta(\eta)$, greater rotation parameter value Ω refers to the higher temperature profile $\theta(\eta)$, and the higher thermal layer width.

Fig. 6 demonstrates that velocity ($f'(\eta)$, $g(\eta)$) and temperature ($\theta(\eta)$) of hybrid nanofluid increases by increasing n in the upper branch. However, the opposite pattern is found in the lower branch.

The effects of Eckert number Ec_1 and Ec_2 on the profiles of temperature are exhibited in Fig. 7. Profiles of temperature rises as Ec_1 and Ec_2 are enhanced for both branches. It is also noticed that the temperature of the hybrid nanofluid boosts quickly when Ec_1 increases as compared to Ec_2.
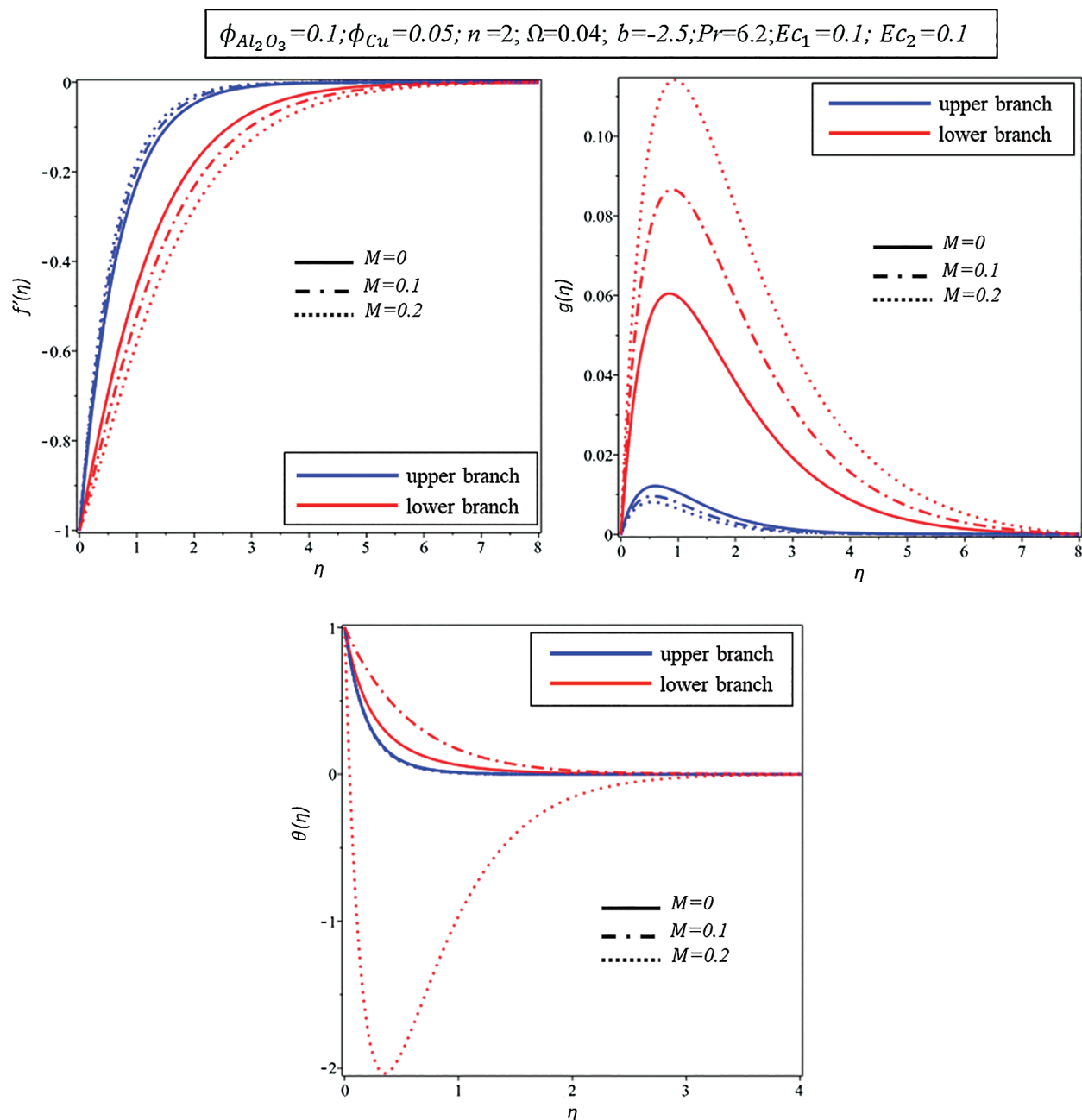

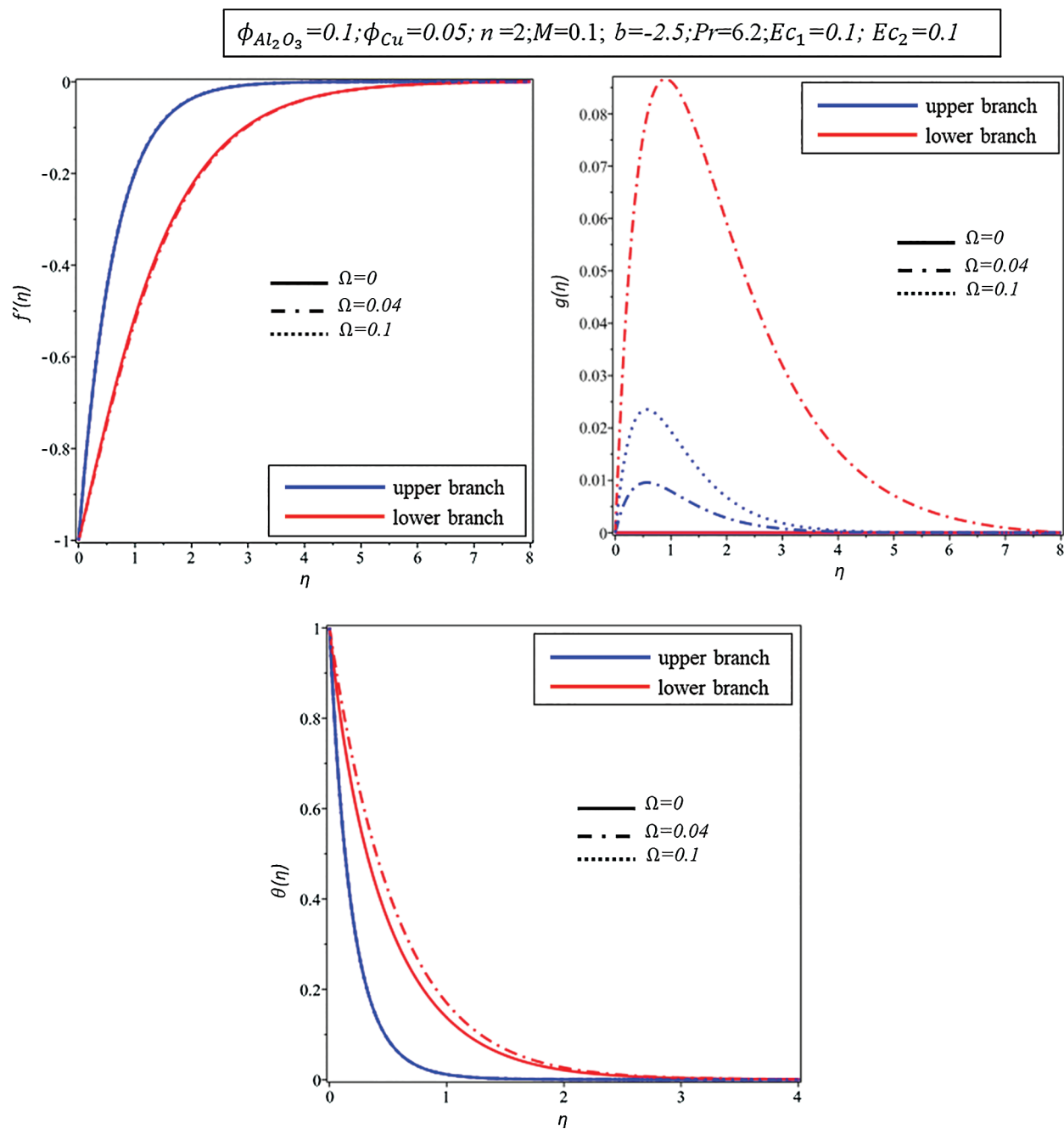Figure 4: Effect of M on various profiles

$$\phi_{Al_2O_3}=0.1; \phi_{Cu}=0.05; n=2; M=0.1; b=-2.5; Pr=6.2; Ec_1=0.1; Ec_2=0.1$$

Figure 5: Effect of Ω on various profiles

Fig. 8 shows the impacts of Ω on the velocity $g(\eta)$ profile. The velocity profiles contain duality in nature when Ω increases. It has been found that the behavior of the velocity profile has the same behavior for the negative and positive values of the rotation (Ω) parameter. Physically, it displays that problem of hybrid nanofluid has a symmetrical solution.
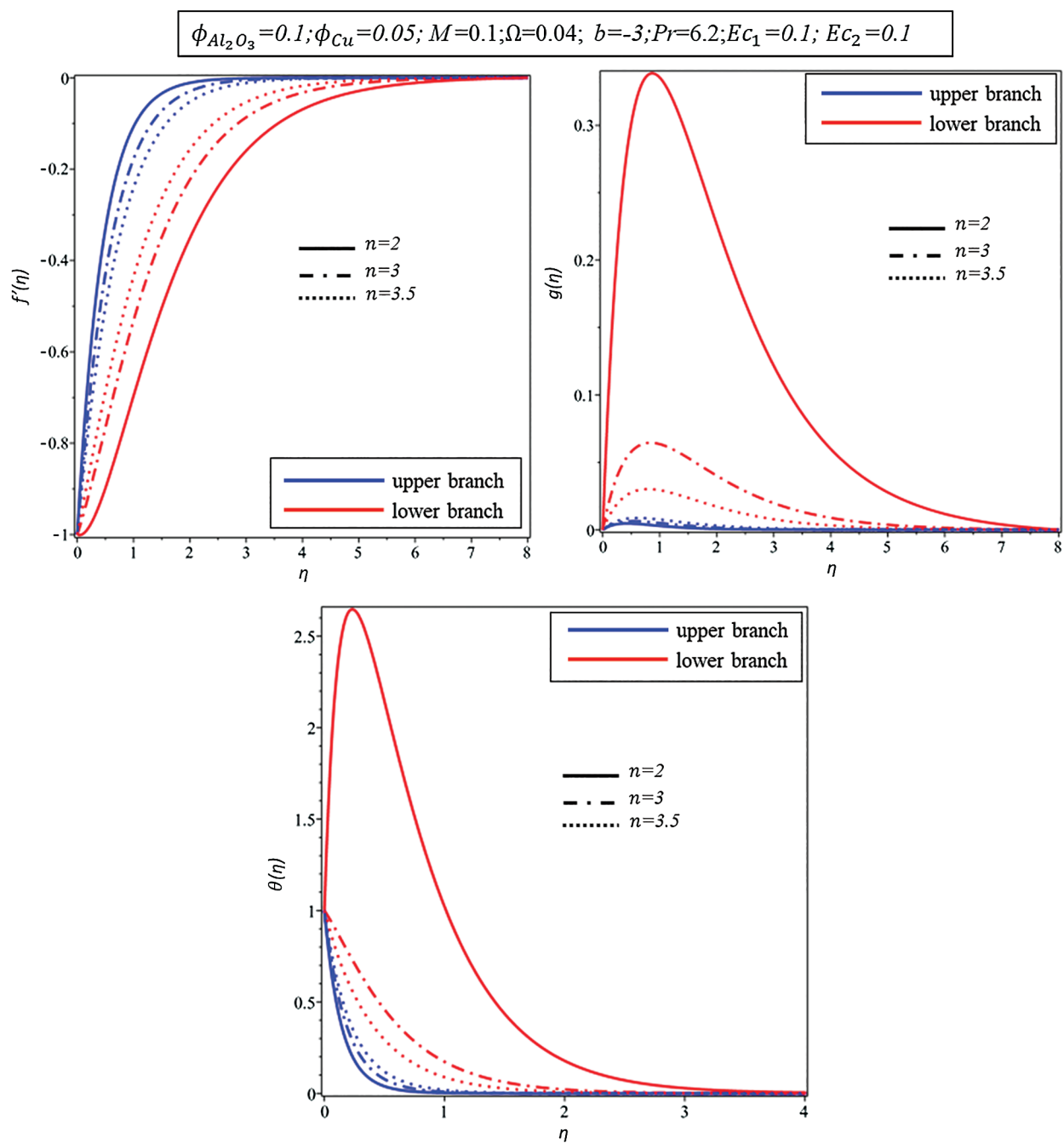
$\phi_{Al_2O_3}=0.1; \phi_{Cu}=0.05; M=0.1; \Omega=0.04; b=-3; Pr=6.2; Ec_1=0.1; Ec_2=0.1$

Figure 6: Effect of n on various profiles
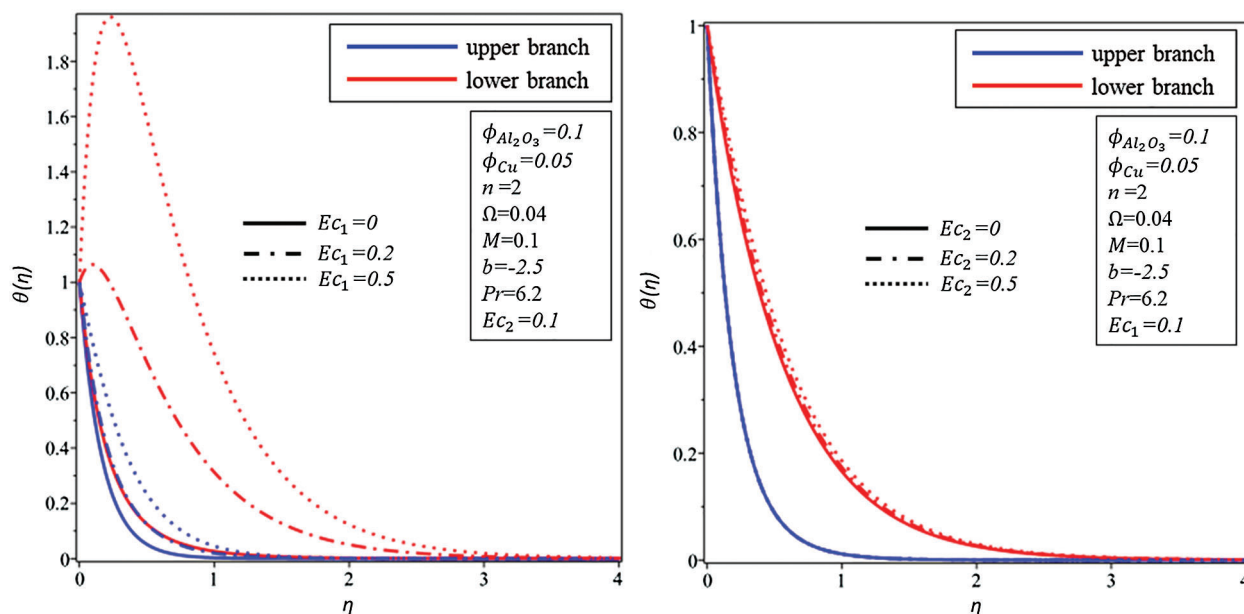
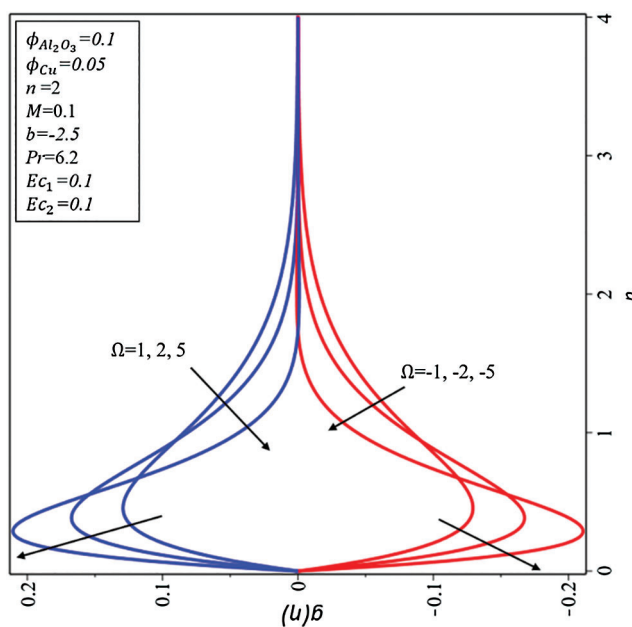**Figure 7:** Effect of Eckert numbers on temperature profile

Figure 8: Effect of Ω on $g(\eta)$

4 Conclusion

In this study, we have considered the flow of rotating MHD of a water-based hybrid nanofluid on a nonlinear shrinking surface. The transformed nonlinear coupled ODEs along with BCs have been numerically examined and computed by employing of *bvp4c* function in Matlab software. Our few main findings on this research are as follows:

1. The heat transfer rate of the hybrid nanofluid is higher than the regular nanofluid.

2. Two branches exist in the case of the higher suction.

3. Numerical outcomes indicated that branches are not unique when $b < b_c$.

4. Temperature and thickness of the thermal layer increase for the higher values of the Eckert number.

5. The thickness of the thermal boundary layer reduces when the Prandtl number increases.

6. The symmetrical nature of branches exists for the solution of the angular velocity.

7. Heat transfer rate increases as the suction increases

8. Dual branches depend on the value of the rotational parameter.

Conflicts of Interest: The authors declare that they have no conflicts of interest to report regarding the present study.

References

[1] S. U. S. Choi and J. A. Eastman, "Enhancing thermal conductivity of fluids with nanoparticles," *ASME Fluids Engineering Division*, vol. 231, pp. 99–105, 1995.

[2] M. Sheikholeslami and R. Ellahi, "Three dimensional mesoscopic simulation of magnetic field effect on natural convection of nanofluid," *International Journal of Heat and Mass Transfer*, vol. 89, pp. 799–808, 2015.

[3] T. Hayat, T. Muhammad, A. Alsaedi and M. S. Alhuthali, "Magnetohydrodynamic three-dimensional flow of viscoelastic nanofluid in the presence of nonlinear thermal radiation," *Journal of Magnetism and Magnetic Materials*, vol. 385, pp. 222–229, 2015.

[4] M. Subhani and S. Nadeem, "Numerical analysis of micropolar hybrid nanofluid," *Applied Nanoscience*, vol. 9, no. 4, pp. 447–459, 2019.

[5] C. Qi, J. Tang, Z. Ding, Y. Yan, L. Guo *et al.,* "Effects of rotation angle and metal foam on natural convection of nanofluids in a cavity under an adjustable magnetic field," *International Communications in Heat and Mass Transfer*, vol. 109, 104349, 2019.

[6] S. Islam, A. Khan, W. Deebani, E. Bonyah, N. A. Alreshidi *et al.,* "Influences of Hall current and radiation on MHD micropolar non-Newtonian hybrid nanofluid flow between two surfaces," *AIP Advances*, vol. 10, no. 5, 055015, 2020.

[7] M. H. Esfe, M. K. Amiri and A. Alirezaie, "Thermal conductivity of a hybrid nanofluid," *Journal of Thermal Analysis and Calorimetry*, vol. 134, no. 2, pp. 1113–1122, 2018.

[8] S. Suresh, K. P. Venkitaraj, P. Selvakumar and M. Chandrasekar, "Synthesis of Al_2O_3–Cu/water hybrid nanofluids using two step method and its thermo physical properties," *Colloids and Surfaces A: Physicochemical and Engineering Aspects*, vol. 388, no. 1–3, pp. 41–48, 2011.

[9] S. A. Devi and S. S. U. Devi, "Numerical investigation of hydromagnetic hybrid Cu–Al_2O_3/water nanofluid flow over a permeable stretching sheet with suction," *International Journal of Nonlinear Sciences and Numerical Simulation*, vol. 17, no. 5, pp. 249–257, 2016.

[10] L. A. Lund, Z. Omar, I. Khan and S. Dero, "Multiple solutions of Cu-$C_6H_9NaO_7$ and Ag-$C_6H_9NaO_7$ nanofluids flow over nonlinear shrinking surface," *Journal of Central South University*, vol. 26, no. 5, pp. 1283–1293, 2019.

[11] L. A. Lund, Z. Omar, J. Raza, I. Khan and E. S. M. Sherif, "Effects of stefan blowing and slip conditions on unsteady MHD Casson nanofluid flow over an unsteady shrinking sheet: Dual solutions," *Symmetry*, vol. 12, no. 3, pp. 487, 2020.

[12] L. A. Lund, Z. Omar, I. Khan and E. S. M. Sherif, "Dual solutions and stability analysis of a hybrid nanofluid over a stretching/shrinking sheet executing MHD flow," *Symmetry*, vol. 12, no. 2, 276, 2020.

[13] L. A. Lund, Z. Omar, J. Raza and I. Khan, "Magnetohydrodynamic flow of Cu-Fe_3O_4/H_2O hybrid nanofluid with effect of viscous dissipation: Dual similarity solutions," *Journal of Thermal Analysis and Calorimetry*, pp. 1–13, 2020, (in Press).

[14] L. Yan, S. Dero, I. Khan, I. A. Mari, D. Baleanu *et al.,* "Dual solutions and stability analysis of magnetized hybrid nanofluid with joule heating and multiple slip conditions," *Processes*, vol. 8, no. 3, 332, 2020.

[15] G. Rasool, T. Zhang and A. Shafiq, "Marangoni effect in second grade forced convective flow of water based nanofluid," *Journal of Advances in Nanotechnology*, vol. 1, no. 1, pp. 50, 2019.

[16] D. Huang, Z. Wu and B. Sunden, "Effects of hybrid nanofluid mixture in plate heat exchangers," *Experimental Thermal and Fluid Science*, vol. 72, pp. 190–196, 2016.

[17] M. N. Rostami, S. Dinarvand and I. Pop, "Dual solutions for mixed convective stagnation-point flow of an aqueous silica-alumina hybrid nanofluid," *Chinese Journal of Physics*, vol. 56, no. 5, pp. 2465–2478, 2018.

[18] J. Sarkar, P. Ghosh and A. Adil, "A review on hybrid nanofluids: Recent research, development and applications," *Renewable and Sustainable Energy Reviews*, vol. 43, pp. 164–177, 2015.

[19] L. A. Lund, Z. Omar and I. Khan, "Quadruple solutions of mixed convection flow of magnetohydrodynamic nanofluid over exponentially vertical shrinking and stretching surfaces: Stability analysis," *Computer Methods and Programs in Biomedicine*, vol. 182, 105044, 2019.

[20] T. Hayat, R. Noureen and T. Javed, "Nonlinear stretching flow with thermal radiation," *Zeitschrift für Naturforschung A*, vol. 65, no. 10, pp. 761–770, 2010.

[21] Z. Shah, T. Gul, S. Islam, M. A. Khan, E. Bonyah *et al.,* "Three dimensional third grade nanofluid flow in a rotating system between parallel plates with Brownian motion and thermophoresis effects," *Results in Physics*, vol. 10, pp. 36–45, 2018.

[22] T. Hayat, F. Haider, T. Muhammad and A. Alsaedi, "Three-dimensional rotating flow of carbon nanotubes with Darcy-Forchheimer porous medium," *PLoS One*, vol. 12, no. 7, e0179576, 2017.

[23] R. K. Tiwari and M. K. Das, "Heat transfer augmentation in a two-sided lid-driven differentially heated square cavity utilizing nanofluids," *International Journal of Heat and Mass Transfer*, vol. 50, no. 9–10, pp. 2002–2018, 2007.

[24] L. A. Lund, Z. Omar, J. Raza and I. Khan, "Triple solutions of micropolar nanofluid in the presence of radiation over an exponentially preamble shrinking surface: Convective boundary condition," *Heat Transfer*, vol. 49, no. 5, pp. 3075–3093, 2020.

[25] L. A. Lund, Z. Omar, I. Khan, D. Baleanu and S. K. Nisar, "Triple solutions and stability analysis of micropolar fluid flow on an exponentially shrinking surface," *Crystals*, vol. 10, no. 4, 283, 2020.